13th International Conference on
Structural Health Monitoring of Intelligent Infrastructure
DOI: 10.3217/978-3-99161-057-1-181

Effects of grout-strand interface modelling on the degradation of external grouted post-tensioning tendons

Belén Vecino[1, 0009-0002-9234-4005], Carlos M.C. Renedo[1, 0000-0003-1014-0878], Luis Chillitupa-Palomino[1, 0009-0001-5274-0436], Iván M. Díaz[1, 0000-0001-9283-5109]

[1]Department of Continuum Mechanics and Theory of Structures, ETSI Caminos, Canales y Puertos, Universidad Politécnica de Madrid, Calle Profesor Aranguren 3, Madrid, 28040, Comunidad de Madrid, Spain

email: b.vecino@alumnos.upm.es, carlos.martindelaconcha@upm.es, luis.cpalomino@upm.es, ivan.munoz@upm.es

ABSTRACT: In recent years, relevant brittle fractures of external grouted post-tensioning tendons in bridges have been reported due to corrosion damage, compromising the structural safety and stability of the bridges. A previous detailed finite element (FE) modelling approach for grouted tendons has been developed by the authors and compared with experimental results presented in the literature, ensuring an accurate reproduction of experimental results by accounting for steel plasticity and large deformations. This modelling approach considered a bonded contact to model the strand-grout interface. That is, an immediate re-anchoring of the strands in the grout is assumed in case of failure and, consequently the influence of the bond stress-slip behaviour is not considered in the modelling approach. This paper presents an alternative FE modelling strategy where the differences with the previous one are: i) the modelling of the strands as beams instead of solid bodies, ii) the presence of the sheathing duct, and iii) a non-linear model to reproduce the strand-grout bond stress-slip behaviour. The objective is to investigate the influence of different models to define the grout-strand interface: a bonded model or a bond stress-slip model, while validating the author's previous FE approach. These models are also compared with the experimental results from the literature. Normal stresses along the strands and in the grout are studied, and degradation curves are derived, that is, the effective tensile force and natural frequencies versus damage (defined as the percentage of broken strands). These degradation curves serve as a key performance indicator of the structural performance of the tendon for structural health monitoring systems, anticipating to severe damage and potentially dangerous scenarios.

KEY WORDS: Damage detection; Corrosion damage; Post-tensioning tendons; Finite element modelling.

1 INTRODUCTION

External post-tensioning tendons are key structural elements in bridge engineering, offering advantages like the ease of inspection, re-tensioning and substitution; however, they are also vulnerable to corrosion. Since the 1990's, relevant brittle fractures of external grouted post-tensioning tendons have been reported in bridges due to corrosion damage [1],[2]. This situation significantly compromises the structural integrity and safety of these bridges.

In externally grouted post-tensioning tendons, strand breakage does not necessarily lead to a significant reduction in the overall tensile force of the tendon. This is because the surrounding grout prevents the movement of the broken strand, effectively re-anchoring it and enabling the transfer of its tensile force to adjacent strands. As a result, the adjacent non-broken strands experience a localised increase of their tensile stress near the breakage region [3]. This stress redistribution occurs over a defined transfer length, which is the distance needed for the strands to nearly recover their original tensile force [3]. However, if a considerable number of strands are affected by corrosion, the resulting stress concentration may exceed the remaining strands' capacity, potentially leading to a brittle failure of the tendon.

Numerical research on the mechanical behaviour of external post-tensioning tendons affected by corrosion remains limited. Aparicio et al. [3] studied the re-anchoring phenomenon in monostrand tendons. A numerical model validated with experimental tests was developed to assess the sensitivity of parameters such as the grout elastic modulus, the mesh, or the friction coefficient in stress redistribution when there is wire breakage. However, they did not consider the constitutive non-linear behaviour of the tendon materials. Subsequently, Vecino et al. [4] (the authors of the present paper) proposed a numerical modelling approach of external grouted post-tensioning tendons to be used within a parametric study to evaluate tendon failure. The grout-strand contact was modelled as bonded (that is, no sliding between them is allowed), but accounting for a prescribed re-anchoring length, plasticity was considered for the high-strength steel of the strands, and the grout was considered perfectly elastic in such a way that the sheathing duct was not explicitly modelled. The modelling approach presented in the previous paper was validated through the experimental results obtained by Lee & Kang [3]. They carried out a laboratory experimental campaign to analyse the variation in dynamic parameters and the tensile force of tendons subjected to progressive corrosion.

Thus, this study focuses on modelling strategies for the grout-strand interface to carry out numerical approaches that are both efficient and accurate. The numerical results obtained are compared against experimental data available in the literature and previous numerical studies performed by the authors, which assume a bonded contact between the strand and the grout. The accuracy of this modelling assumption is assessed to determine whether it serves for practical purposes or if a more complex contact approach, such as incorporating a non-linear bond stress–slip relationship, is required.

Establishing an appropriate modelling strategy for grouted tendons and the re-anchoring behaviour of strands is essential

DOI: 10.3217/978-3-99161-057-1-181

for the reliable analysis of their structural performance. Accurate numerical models can support comprehensive risk assessments in the context of structural health monitoring (SHM) and serve as a tool for engineers and practitioners to complement inspections and prevent safety-critical situations.

The present paper is organised as follows. Section 2 provides a detailed description of the finite element (FE) model developed here and present a former model previously validated by the authors to study tendon degradation. Section 3 provides a discussion of the results obtained by the proposed modelling approach and using different grout-strand contact laws. Finally, Section 4 outlines some conclusions from the study.

2 FINITE ELEMENT MODEL

2.1 Experimental tests carried out by Lee & Kang

The experiment conducted by Lee & Kang [3] is used as a reference to compare their experimental results and the numerical results obtained in this investigation in terms of the degradation curves, which are: i) the tensile force with damage, and ii) the natural frequencies with damage. Damage is defined as the quotient between the number of broken strands and the total number of strands of the tendon: $D = N_B/N$, where N_B is the number of broken strands and N is the total number of strands.

This experiment was also used to validate the detailed FE modelling approach previously carried out by the authors [2], whose results on degradation curves are also contrasted with the ones obtained in this paper.

The Lee & Kang experiment stresses a 10 m tendon at approximately 70% of the ultimate load of a prestressing strand. Then, five strands are broken successively by accelerated corrosion in 24 hours. To carry out the breakage of the strands, the grout is retired in the 30 cm central section, leaving the strands exposed.

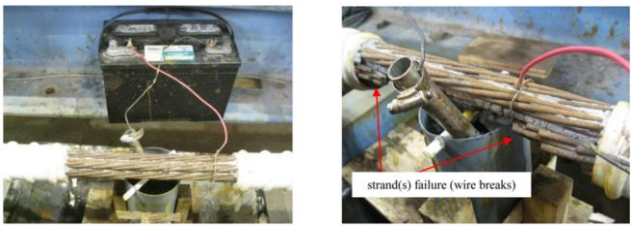

Figure 1. Strands subjected to accelerated corrosion [3].

2.2 FE model 1: 3D elements and bonded strand-grout interface

The Lee & Kang experiment was reproduced by the authors [4] using a FE detailed model of a seven-strand tendon surrounded by grout, except for the central section of 60 cm, which is modelled without grout to reproduce the Lee & Kang experiment, and to consider the re-anchoring length. This parameter was prescribed in the model due to the grout-strand contact considered, which will be explained hereafter.

The stress state reached by the stressing of the strands is modelled by a thermal load, at 70% ultimate stress, f_{pu}, which is 1900 MPa. Then, the stressing force of the tendon is 1241 kN. The strands' breakage due to corrosion damage is represented by the elimination of elements. The FE model was developed in ANSYS Mechanical using 3D SOLID185 elements for the grout and the steel strands. The duct (which has the main function of confining the grout to prevent its breakage) was neglected by assuming a perfectly elastic material for the concrete with a higher density (to include the duct weight). Sweep meshing method was used so that the positions of the nodes of the grout match with those of the strands in each section. Both ends of the seven strands were modelled with fixed support, that is, rotation and translation were restrained at both supports. A linear elastic surface-to-surface contact model was assumed between the grout and the strands; specifically, a bonded contact, which prevents separation and sliding. The bonded contact model does not capture the re-anchoring effect; a re-anchoring length had to be predefined in the model to simulate this behaviour. Plasticity of steel strands is considered. The elastoplastic model used presents the following characteristics: i) Bilinear isotropic hardening law, defined in Table 1, ii) Von Mises yield criterion, and iii) Associated flow rule.

Table 1. Bilinear isotropic hardening model parameters.

E_s [GPa]	f_{py} [MPa]	ε_{py} [%]	f_{pu} [MPa]	ε_{pu} [%]
195.5	1760	0.9	1900	6

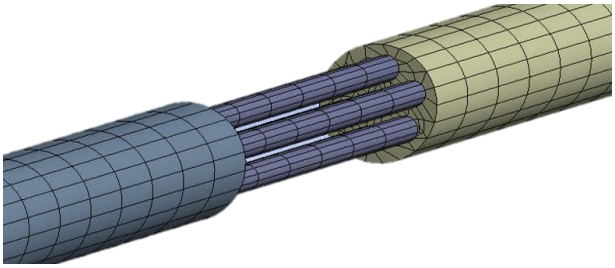

Figure 2. FE tendon model developed previously by the authors in [4] (FE model 1).

2.3 FE model 2: beam elements for strands and non-linear springs for the interface

The bonded contact employed in the FE model 1 for the grout-strand interface may not accurately capture the re-anchoring phenomenon, as this process involves bond mechanisms such as adhesion, friction, and mechanical interlock [6]. A bond stress-slip law has been proposed and validated by Wang et al. for strands. Thus, a new modelling approach that considers a bond stress-slip law to model the strand-grout interface is developed. The implementation of this law in the model eliminates the need to introduce the re-anchoring length as an input parameter, as in the FE model 1, allowing it to be intrinsically determined.

The Model Code [7] proposes a bond stress-slip relationship for ribbed bars, considering the bond stresses between concrete and reinforcing bar for pull-out. This relationship is defined in Figure 3 and its defining parameters are listed in Table 2.

DOI: 10.3217/978-3-99161-057-1-181

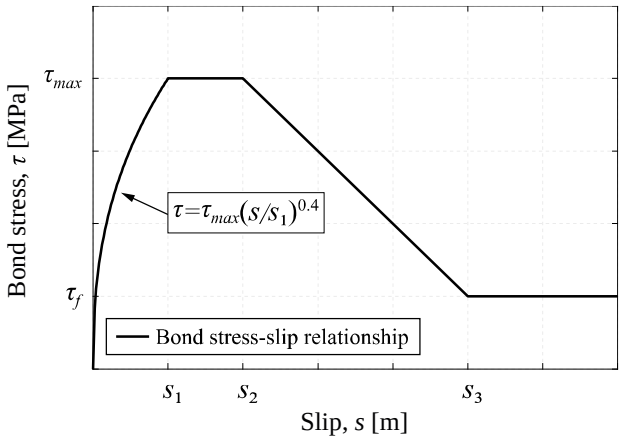

Figure 3. Bond stress-slip relationship [7].

Table 2. Parameters defining the bond stress–slip relationship [7].

τ_{max}	τ_f	s_1	s_2	s_3
$2.5\sqrt{f_{cm}}$	$0.4\,\tau_{max}$	1 mm	2 mm	c_{clear}

Parameter f_{cm} is the concrete compressive strength (a typical value of 30 MPa is considered), and c_{clear} represents the spacing between the ribs of a deformed bar. Considering the similarity in bond behaviour between steel strands and deformed bars embedded in concrete, the parameter s_3 is defined as half of the distance between the concrete interlock region and the adjacent wires [8], and it is taken as 10 mm.

To introduce the bond stress-slip law in the FE model, non-linear springs are defined in every grout-strand coincident node. The elements used to create the non-linear springs are COMBIN39, with one degree of freedom in the longitudinal direction. COMBIN39 is defined by two nodes and a non-linear generalised force-deflection relationship.

The main purpose of this paper is to validate and critically discuss the interface modelling approach developed previously by the authors when considering bonded behaviour (FE model 1) [4]. For that, a new approach to numerically model the Lee and Kang experimental campaign has been developed (FE model 2). This new approach differs from the previous one in the following aspects:

1) Modelling of the HDPE sheathing duct, which is considered elastic. 3D SOLID186 elements are used for the duct, and the duct-grout contact is modelled as bonded. The grout is also modelled with these elements.
2) BEAM188 elements are used to model the strands. This simplifies the introduction of non-linear springs node-to-node to model the grout-strand interface. Also, considering beams for the strands reduces considerably the number of nodes and elements of the model, reducing the computational demand as well, which is one of the main limitations of the previous modelling approach.
3) Considering a non-linear bond stress-slip model to characterise the strand-grout interface. The Model Code bond stress-slip is introduced using non-linear springs (COMBIN39) in the longitudinal direction, whereas linear springs (COMBIN14) of high stiffness (k = 10^{12} N/m) are modelled in the transversal directions. The first branch of the bond stress-slip model (from s=0 to s=s_1) is considered linear for simplification.

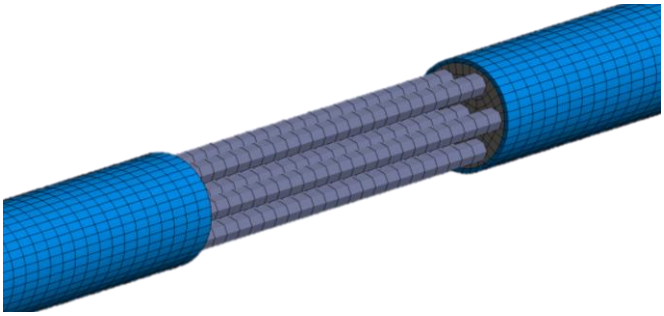

Figure 4. FE tendon model developed (FE model 2).

The differences between the modelling approaches are compiled in Table 3.

Table 3. Comparison of modelling approaches: FE model 1 and FE model 2.

	Sheathing duct	Strand elements	Strand-grout interface
FE model 1 [4]	Not modelled	SOLID186	Bonded contact
FE model 2	SOLID186 elements	BEAM188	Non-linear springs (bond stress-slip/bonded)

Then, four different results are compared:

(i) Lee and Kang experimental results.
(ii) FE model 1 with bonded contact between strands and grout.
(iii) FE model 2 with bonded contact between strands and grout.
(iv) FE model 2 with non-linear bond stress-slip behaviour.

2.4 Analysis description

A non-linear static analysis by load steps is performed. A sparse direct solver and the Newton-Raphson algorithm with convergence in forces, displacements, and moments are used. The non-linearity is caused by the activation and deactivation of elements. The influence of strands' plasticity, large displacement analysis, the grout-strand contact modelling (re-anchoring effects), and the mechanical properties of the grout on the FE modelling are studied. The FE analysis follows these steps (Figure 5):

i) Stressing of the strands by applying a thermal load. The stressing of the strands was executed at 70% of their ultimate stress, f_{pu}. The temperature decrease ΔT is equal to:

$$\Delta T = \frac{0.7\,f_{pu}}{E_s\,\alpha}, \quad (1)$$

where E_s is the elastic modulus of the strands, and α is the thermal expansion coefficient, taken as $1.2{\cdot}10^{-5}$ °C^{-1}.

ii) Activation of the grout to simulate injection.

DOI: 10.3217/978-3-99161-057-1-181

iii) Successive breakage of five strands in five different steps by eliminating elements. The order of strand breakage is from 1 to 5, the strands numeration is illustrated in Figure 5.

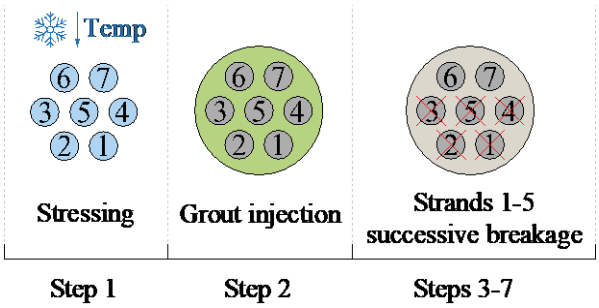

Figure 5. Steps of the FE non-linear static analysis performed.

Furthermore, a modal analysis is performed after each strand breakage step to assess the progressive reduction in the tendon's natural frequencies, which are useful as performance indicators (PIs) when performing vibration-based SHM of these elements. The characteristic stress state corresponding to each load step is incorporated into the modal analysis through the application of a preload state.

3 RESULTS DISCUSSION

3.1 Tensile force degradation with damage

The evolution of tensile force, T, with damage, D, in the anchorage (outside the transfer length) is shown in Figure 6. The re-anchoring effect is captured by the proposed modelling approach (FE model 2), with a similar trend to the experimental and previous numerical results (FE model 1). It must be noted that the re-anchoring length in the FE model 1 was an adjusted parameter to replicate the experimental results, whereas in the FE model 2, it is a result of the implemented contact law. Thus, FE model 2 can replicate the phenomenological behaviour without requiring any preliminary calibration, as opposed to FE model 1. However, the differences observed in the most recent modelling approach compared to the previous one are noticeable. This may be due to modelling the strands as beam elements instead of solid bodies, which may not adequately capture the internal stress distribution within the strand volume.

When comparing the two grout-strand interface models (represented by the green and blue curves), the results are almost identical, indicating that the influence of the interface model used does not affect the accuracy of the results in reproducing the re-anchoring of the strands. However, these results also suggest that the interface modelling for ribbed bars exhibits greater stiffness compared to that for strand re-anchoring in grout.

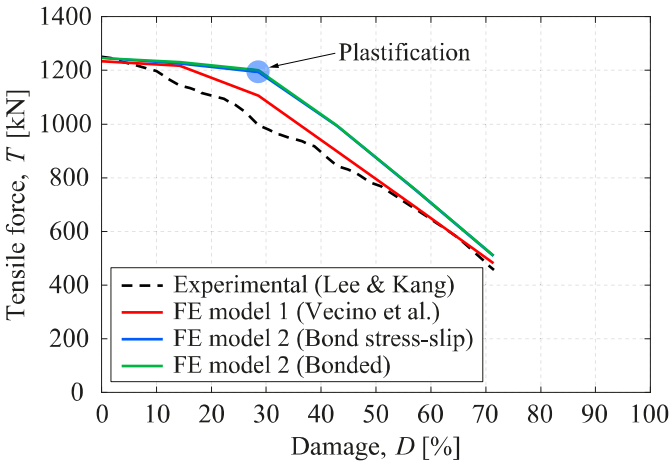

Figure 6. Tensile force degradation with damage.

3.2 Natural frequencies degradation with damage

The evolution of the first four natural frequencies, f_i, of the tendon as damage progresses is also analysed in Figure 7. In this figure, $f_{i,exp}$ refers to the frequencies obtained in the Lee & Kang experiment, $f_{i,num}$ to the ones corresponding to the FE model 1, whereas the other two frequency groups refer to the FE model 2 with bonded and bond stress-slip models.

A behaviour similar to that observed in the tensile force degradation is noted when comparing the FE model results with the experimental data. While the overall trend is consistent, the natural frequencies predicted by the models are slightly higher than the experimental values, and the new modelling approach exhibits more pronounced discrepancies. However, the results obtained using the different interface models remain phenomenologically similar.

The degradation of natural frequencies becomes more pronounced at higher damage levels and is more significant in absolute terms for the higher modes. Accurately quantifying the absolute reduction in frequencies is important for their effective use as a PI in structural health assessment [4].

DOI: 10.3217/978-3-99161-057-1-181

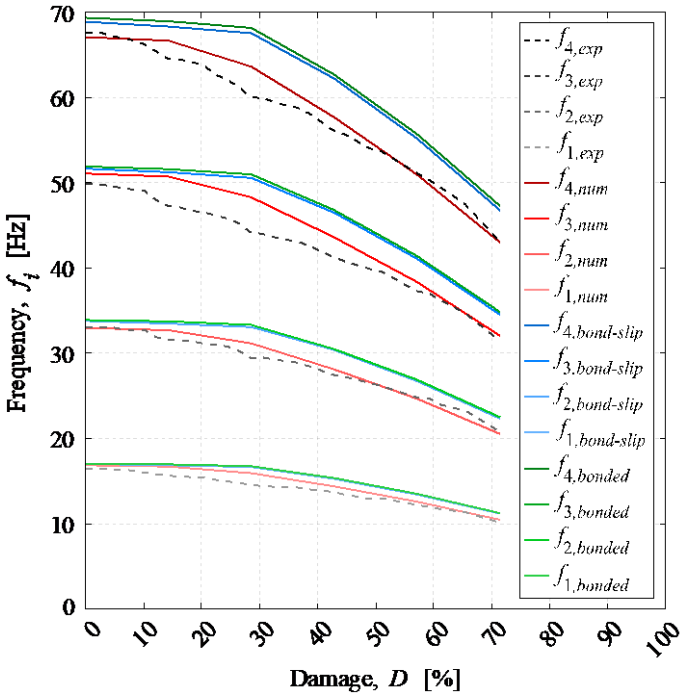

Figure 7. Frequency degradation with damage.

3.3 FE model 2: normal stresses along the strands

Two strands are considered for the study of the normal stresses along the strands: i) Strand 5, which is the central strand and is the last to break (Figure 8), and ii) Strand 6, which is a central that remains continuous throughout the entire analysis (Figure 9). The two interface models (bonded and bond stress-slip) are also compared.

Strand 5 exhibits a local increase in stresses as a result of the successive breakage of strands, becoming more pronounced as damage progresses, with fewer continuous strand remaining to carry the stresses of the broken ones. Additionally, the re-anchoring effect is observed in both models, where, in regions distant from the vicinity of breakage, the stress along the strand remains constant. Along the re-anchoring length, a transition occurs between the constant stress away from the breakage zone and the increased stress near the breakage. Both models effectively represent the re-anchoring effect; however, the primary difference lies in the re-anchoring length. The bond stress-slip model (Figure 8 (a)) shows a larger re-anchoring length, approximately 1.9 m, with a smoother transition in stresses, while the bonded model (Figure 8 (b)) exhibits a shorter re-anchoring length, around 0.9 m. This results in a difference of approximately 1 m in the re-anchoring length between the two models.

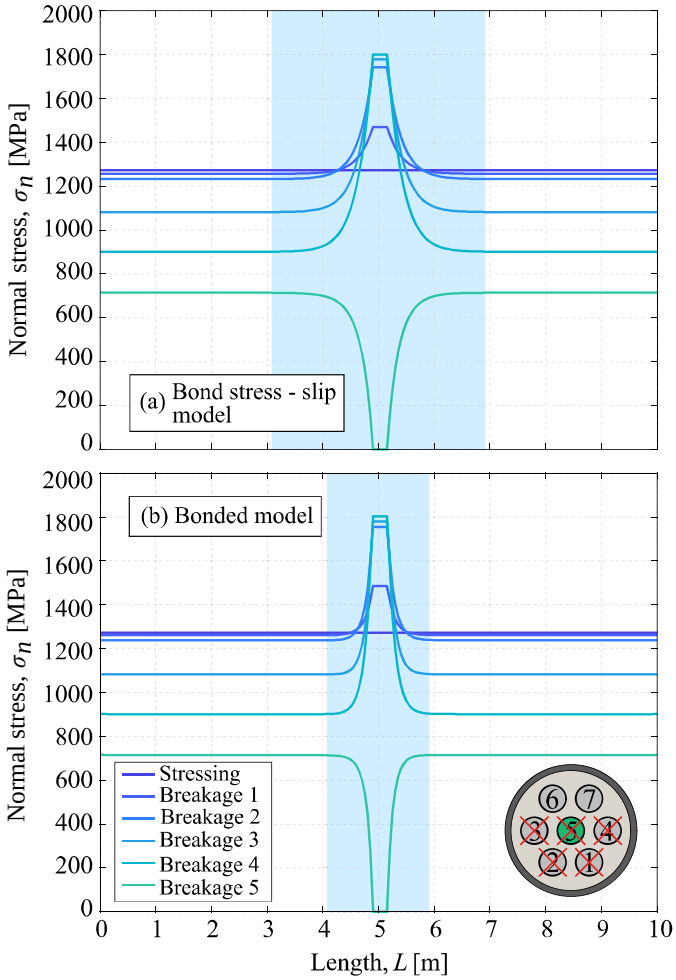

Figure 8. Normal stresses along strand 5 for different strand-grout interface modelling. (a) Bond stress-slip model. (b) Bonded model. Blue shadowed areas indicate the re-anchoring length.

Similar results are observed for strand 6. The stress evolution along the strand demonstrates the stress redistribution resulting from the successive breakage of strands. In a similar manner as for strand 5, the re-anchoring length is greater for the bond stress-slip model, where it is 2.2 m, compared to 1.9 m for the bonded model. The difference of 0.3 m is smaller in this case, as this strand does not break during the analysis. Given the exponential nature of the re-anchoring phenomenon, the re-anchoring length is a highly sensitive parameter to the point at which complete re-anchoring is achieved.

DOI: 10.3217/978-3-99161-057-1-181

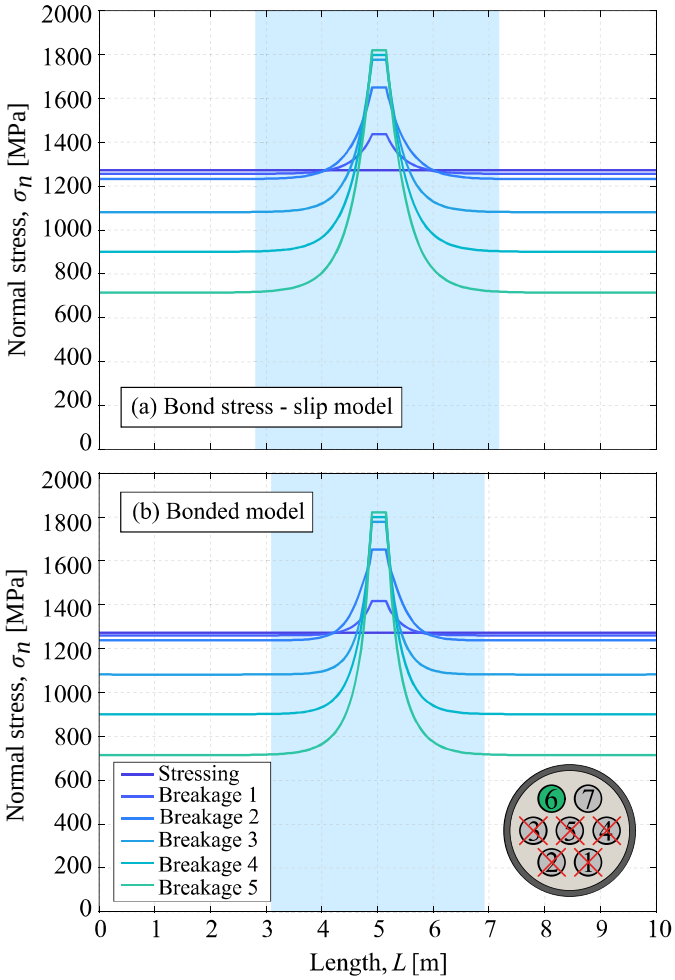

Figure 9. Normal stresses along strand 6 for different strand-grout interface modelling. (a) Bond stress-slip model. (b) Bonded model. Blue shadowed areas indicate the re-anchoring length.

3.4 FE model 2: normal stresses in the grout

The normal stresses in the grout as a function of damage are shown in Figure 10 for the two interface models studied, obtaining similar results for both. The grout normal stresses are analysed to characterise the grout's mechanical response, given that it has been modelled as perfectly elastic, which may not accurately represent the typical grout constitutive behaviour.

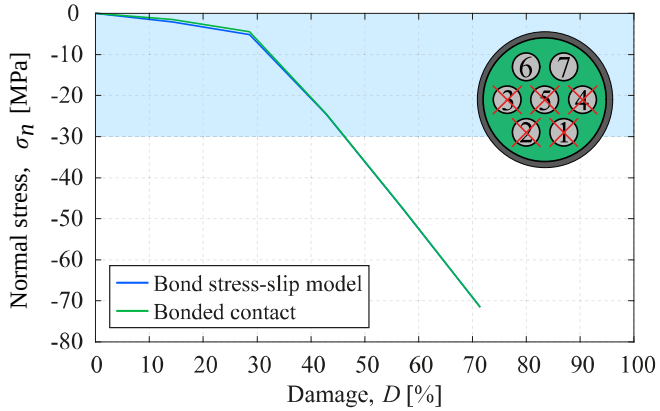

Figure 10. Normal stress in the grout with damage progression.

The compressive strength of the grout is 30 MPa, this value is reached for approximately a 45% of damage. Beyond this point, crack formation and propagation are expected to start. For the maximum damage value studied (71%), the stresses reach 70 MPa, which are considerably high, more than twice the compressive strength of the material. These stress values are not realistic; this highlights the limitations of the linear elastic assumption and suggests the need for a more accurate non-linear constitutive model.

4 CONCLUSIONS

The following conclusions are drawn:

1. The tensile force and the natural frequencies serve as PIs for damage detection within the context of SHM, provided that their degradation due to damage is accurately reproduced numerically. It can support early identification of deterioration mechanisms, complement fieldwork, and contribute to a more effective maintenance.
2. The new FE modelling approach shows discrepancies compared to the authors' previous numerical results, which may be attributed to the modelling of strands as beam elements instead of solid bodies. This also may explain the increased deviations from experimental results. However, the use of beam elements reduces computational demands, which was a limiting factor in the previous modelling strategy.
3. The influence of different literature-based grout-strand interface models is minimal compared to a bonded interface behaviour, as the results obtained are nearly identical. The primary difference lies in the re-anchoring length, which is approximately 1 m longer for broken strands when using the bond stress-slip model.
4. The interface models used to simulate ribbed bar pull-out may not be directly applicable to prestressing strands in external grouted tendons. The results indicate that the stiffness of the grout-strand interface may be considerably lower.
5. Future research aimed at improving the FE modelling of grouted tendons should focus on incorporating a non-linear constitutive model for the grout and a more realistic bond stress-slip behaviour with much less stiffness than those used for internal tendons or rebars.
6. In previous work [4], the authors applied the modelling strategy to conduct a parametric study to identify the critical number of strands broken leading to tendon failure. A reliable and efficient FE modelling approach can serve as a valuable tool in SHM applications, enabling risk assessment and early damage detection.

ACKNOWLEDGMENTS

Research project PID2021-127627OB-I00 funded by MCIN/AEI/10.13039/501100011033/FEDER, EU. Belén Vecino acknowledges the Fundación Agustín de Betancourt for the financial support provided for the development of her doctoral thesis.

DOI: 10.3217/978-3-99161-057-1-181

REFERENCES

[1] Kretz T, Lacombe J-M, Godart B. (2007). Note de sensibilisation sur les ouvrages existants à précontrainte extérieure protégée par du coulis de ciment au contact des armatures. Sétra.
[2] Lau, K., Permeh, S., & Vigneshwaran, KK. (2016). Corrosion of post-tensioned tendons with deficient grout: Final report. Florida Department of Transportation.
[3] Lee JK, Kang JW. (2019). Experimental evaluation of vibration response of external post-tensioned tendons with corrosion. KSCE Journal of Civil Engineering, 23, 2561–2572. https://doi.org/10.1007/s12205-019-0735-5.
[4] Aparicio J, Hoang T, Cumunel G, Forêt G, Jeanjean Y, Saint Martin JC. (2023). Experimental and numerical study on the re-anchoring of wire in grouted prestressed tendons. In: Istanbul IABSE Symposium (ISTBR 2023) LONG SPAN BRIDGES.
[5] Vecino B, Renedo CMC, García-Palacios JH, Díaz IM. (2025). Degradation modelling of external grouted post-tensioning tendons: Numerical assessment under corrosion conditions. Engineering Structures, 327, 119620.
[6] Wang L, Yuan P, Zhang X, Dong Y, Ma Y, Zhang J. (2019). Bond behavior between multi-strand tendons and surrounding grout: Interface equivalent modeling method. Construction and Building Materials, 226, 61–71. https://doi.org/10.1016/j.conbuildmat.2019.07.242.
[7] Fédération Internationale du Béton. (2020). Model Code 2020: Final version. Vol. 1–2.
[8] Wang L, Zhang X, Zhang J, Yi J, Liu Y. (2017). Simplified model for corrosion-induced bond degradation between steel strand and concrete. Journal of Materials in Civil Engineering, 29(4), 04016257.